
**Liquid Crystals**
Publication details, including instructions for authors and subscription information:
http://www.informaworld.com/smpp/title~content=t713926090

# Stationary states of the surface stabilized ferroelectric liquid crystal layers in electric field

G. Derfel[a]
[a] Institute of Physics, Technical University of łódź, łódź, Poland

**To cite this Article** Derfel, G.(1990) 'Stationary states of the surface stabilized ferroelectric liquid crystal layers in electric field', Liquid Crystals, 8: 3, 331 — 343
**To link to this Article: DOI:** 10.1080/02678299008047351
**URL:** http://dx.doi.org/10.1080/02678299008047351

LIQUID CRYSTALS, 1990, VOL. 8, NO. 3, 331–343

# Stationary states of the surface stabilized ferroelectric liquid crystal layers in electric field

by G. DERFEL
Institute of Physics, Technical University of Łódź, 93-005 Łódź, Poland

(*Received 16 January 1990; accepted 21 April 1990*)

Stationary states of surface stabilized ferroelectric liquid crystal layers in an electric field are analysed by use of the Taylor expansion method based on catastrophe theory. Two kinds of director distribution within the flat smectic layers are taken into account: the uniform and the presplayed one. The butterfly catastrophe describes the properties of the cells correctly. The results have a qualitative character. Two categories of transitions can be predicted: switching between stable states characterized by opposite uniform orientations of the polarization vectors, and deformation of the director field which relaxes after removing the field. The threshold field strengths are found and the role of the system parameters is investigated.



## 1. Introduction

Ferroelectric liquid crystals offer a very attractive possibility for applications in display devices invented by Clark and Lagerwall [1]. Electrooptic effects utilized in the displays are being studied intensively both experimentally and theoretically. The switching processes usually involve the nucleation and growth of domains bounded by disclination loops. These complicated phenomena require a two dimensional analysis at least, and have so far been treated theoretically in an approximate way [2, 3]. The stationary states can be considered as one dimensional problems. They were investigated from the viewpoint of elastic continuum theory, e.g. in [4–8]. A one dimensional approach was also applied to the dynamics of the switching process in which director rotation was assumed [9–12]. Such an effect was observed [13], and can yield high quality displays [14]. Several variants of the ferroelectric cells have been examined, using different assumptions concerning the director distribution. In this paper, the qualitative characteristic of the static properties of the ferroelectric liquid crystal layer, due to various geometric and material parameters, is obtained by the method based on catastrophe theory [15]. This method is valuable in determining the number and kind of critical points of the function considered. It predicts the equilibrium states of the system and investigates their stability. It allows us to recognize the character of the critical phenomena which can take place in external electric fields; its application has been described in [16, 17, 18].

Two simple systems consisting of flat smectic layers are taken into account: a structure (tilted or not) with a uniform director field resulting from non-polar surface interactions and a structure with a presplayed director resulting from polar surface interactions. The helicoidal structure is assumed to be suppressed by the boundary surfaces. To aid in the proper interpretation of further results, the oversimplified model of highly stiff chiral smectic C is first considered in §2. The method used in this paper is presented in §3. Geometries with the smectic layers perpendicular to the

0267-8292/90 $3.00 

boundary plates are considered in §4. In §5 the effect of layer tilt is described. Section 6 contains a short discussion of the result. The usual approximations are made: the biaxiality of the chiral smectic C phase is neglected, no influence of the electric field on the smectic C tilt angle, $\omega$, and no distortion of the smectic layers are taken into account. The effect of the space charge, due to non-zero divergence of the spontaneous polarization, is included approximately into the electric field strength. However, for tilted smectic layers, $\nabla \mathbf{P} = 0$ is assumed in order to avoid calculational complexity.

## 2. The simplified model

The attractive bistability of the surface stabilized ferroelectric liquid crystal displays is based on a suitable interaction between the liquid crystal and the boundary surfaces. This interaction can be described by the surface energy

$$G = -\gamma_1(\hat{\mathbf{P}} \cdot \hat{\mathbf{s}})^2 - \gamma_2 \hat{\mathbf{P}} \cdot \hat{\mathbf{s}}, \tag{1}$$

where $\hat{\mathbf{P}} = \mathbf{P}/|\mathbf{P}|$ and $\hat{\mathbf{s}}$ is the outward surface normal unit vector. The coefficients $\gamma_1$ and $\gamma_2$ describe the non-polar and polar interactions, respectively. The role of the curvature elasticity of the liquid crystal is not crucial for the principle of operation of the display. This is exemplified by the simple model in which the very stiff material stabilized by non-polar interactions ($\gamma_2 = 0$), is taken into account. In order to retain only the essential features of the effect, the electric energy due to the dielectric anisotropy is neglected in comparison to the energy due to the spontaneous polarization. The smectic layers are parallel to the $yz$ plane and perpendicular to the boundary plates which are placed at $z = \pm d/2$. The state of the cell is completely determined by the angle $\phi$, common for the whole volume, measured anticlockwise between $\mathbf{P}$ and the $z$ axis (see figure 1 ($a$)).

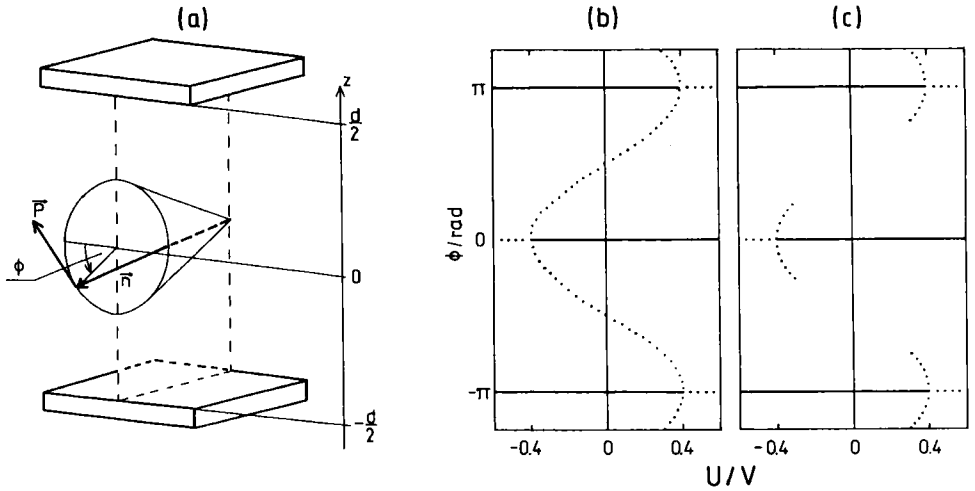


Figure 1. The deformation of an infinitely stiff material. ($a$) The geometry of the stiff liquid crystal layer. ($b$) The angle $\phi$ as a function of the applied voltage $U$ obtained analytically. ($c$) The set of dual cusp catastrophes equivalent to the analytical solution. $d = 2 \times 10^{-6}$ m, $P = 1 \times 10^{-4}$ C/m$^2$, $\gamma_1 = 1 \times 10^{-5}$ N/m (full line, minima: dotted line, maxima).

The energy per unit area of such a sample is given by

$$G = -dPE\cos\phi - 2\gamma_1\cos^2\phi. \tag{2}$$

It possesses extremes for

$$\phi = \pm k\pi, \tag{3}$$

and for

$$\phi = \pm\arccos(-dPE/4\gamma_1) \pm k\pi, \tag{4}$$

where $k$ is zero or integer. The equilibrium states are realized for the solutions (3) but only in suitable ranges of the electric field strength (see figure 1 (*b*)). The transitions between two equilibrium states, e.g. $\phi = 0$ and $\phi = \pi$ occur discontinuously at threshold fields determined by

$$E_c = \pm 4\gamma_1/dP. \tag{5}$$

The same problem can be resolved by use of the power expansion of free energy of the layer in terms of $\phi$ in the vicinity of $\phi = 0$; namely

$$G = a_2\phi^2 + a_4\phi^4 + \ldots, \tag{6}$$

where

$$a_2 = dPE/2 + 2\gamma_1 \tag{7}$$

and

$$a_4 = -dPE - 16\gamma_1. \tag{8}$$

A degenerate critical point exists at $E_c = -4\gamma_1/dP$ and $a_4$ is always negative at this point. Therefore we have to deal with the dual cusp catastrophe. The analogous results are obtained for other critical points determined by $k \neq 0$ in equation (3). The dual cusps due to each of them form a sequence suggested by figure 1 (*b*) and shown in figure 1 (*c*). In some more complicated cases, which are considered in the following sections, a similar sequence of suitable catastrophes is realized resulting in bistability of the layer.

## 3. Method

The deformation of the director field in the layer is modelled by a simple function of three angles, which are required for the determination of the director position at the top boundary, bottom boundary and inside the layer. They are denoted by $\chi$, $\psi$ and $\xi$, respectively. The function should represent all of the essential topological features of the real director distribution. By use of this model function, the approximate free energy $G(\chi, \psi, \xi)$ per unit area of the sample is derived. The critical points of $G$ are found, i.e. the points $(\chi, \psi, \xi)$ for which the first derivatives vanish. The degeneracy of these points is investigated. If the determinant of the matrix of the second derivatives $\mathbf{H}$,

$$\mathbf{H} = \begin{bmatrix} \dfrac{\partial^2 G}{\partial\chi^2} & \dfrac{\partial^2 G}{\partial\chi\,\partial\psi} & \dfrac{\partial^2 G}{\partial\chi\,\partial\xi} \\ \dfrac{\partial^2 G}{\partial\psi\,\partial\chi} & \dfrac{\partial^2 G}{\partial\psi^2} & \dfrac{\partial^2 G}{\partial\psi\,\partial\xi} \\ \dfrac{\partial^2 G}{\partial\xi\,\partial\chi} & \dfrac{\partial^2 G}{\partial\xi\,\partial\psi} & \dfrac{\partial^2 G}{\partial\xi^2} \end{bmatrix}, \tag{9}$$

can be made to vanish by a suitable choice of parameters (e.g. the strength of the electric field), then the critical point considered is degenerate, and the system has some interesting properties in its vicinity. The energy $G$ is expanded in a Taylor series in the neighbourhood of the critical point

$$G = \sum_{i=0}^{\infty} \sum_{j=0}^{\infty} \sum_{k=0}^{\infty} a_{ijk} \chi^i \psi^j \xi^k. \tag{10}$$

After proper normalization, the expanded function $G$ can be reduced to one of the catastrophes. The normalization procedure includes the diagonalization of the matrix **H** and elimination of the inessential variables [15]. Diagonalization is carried out by use of the transformation

$$\left.\begin{aligned} \chi &= c_{11}u + c_{12}v + c_{13}w, \\ \psi &= c_{21}u + c_{22}v + c_{23}w, \\ \xi &= c_{31}u + c_{32}v + c_{33}w. \end{aligned}\right\} \tag{11}$$

The coefficients of the transformation are, in general, found numerically, as the equations leading to them are of third order. Among variables $u$, $v$, $w$, these are essential, for which the second derivatives vanish at the critical point and for the critical set of parameters. In the cases considered later there is only one essential variable. The free energy $G$ is then equivalent to a function

$$\begin{aligned} G = {} & (\partial^2 G/\partial r^2|_{\text{crit. point}})\, r^2 + (\partial^2 G/\partial s^2|_{\text{crit. point}})\, s^2 \\ & + a_1 t + a_2 t^2 + a_3 t^3 + a_4 t^4 + a_5 t^5 + a_6 t^6, \end{aligned} \tag{12}$$

where $r$ and $s$ denote the inessential variables and $t$ the essential one. The critical behaviour of the system is described sufficiently by the expansion in $t$. The coefficients of this expansion are derived during the normalization procedure [15] and are expressed by $a_{ijk}$ and $c_{ij}$. Only the even coefficients are present if the smectic layers are not tilted. Their complicated form makes the analytical consideration of the role of system parameters impossible; numerical examples must be studied for this purpose. Also the truncation of the Taylor series is made after numerical checking which coefficient cannot be made to vanish for any set of typical parameters for the chiral smectic C phase. For the deformations due to the coupling of the spontaneous polarization with the electric field, the coefficient $a_6$ is the first which does not vanish at the threshold. It means that terms of order higher than six may be disregarded, and that the butterfly catastrophe is suitable for the description of the system in the vicinity of the corresponding critical point. For the deformations which have a dielectric origin, the first non-vanishing coefficient at the threshold is $a_4$. The series can be truncated at the fourth term and the cusp catastrophe results.

The dependence of $\chi$, $\psi$ and $\xi$ on the electric field strength or on the applied voltage is found by minimizing $G$ and application of transformation (11). Several distinct cases of the $\chi(E)$, $\psi(E)$ and $\xi(E)$ functions are described. They are obtained for some sets of system parameters which are plausible in practice.

## 4. Smectic layers perpendicular to the boundary plates

The geometry of this structure is shown in figure 2. The director distribution is described by the azimuthal angle $\Phi(z)$ and the function $\Phi(z)$ can be expressed as a sum

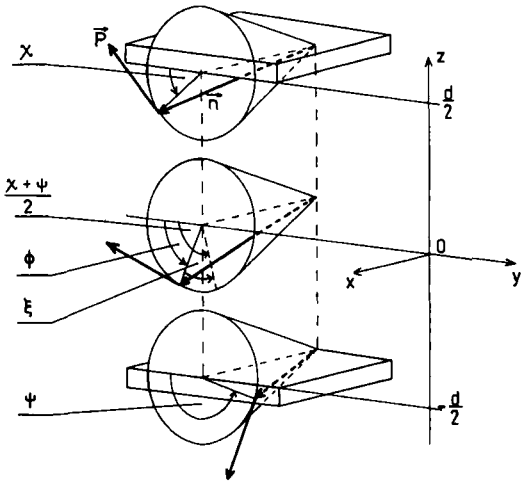


Figure 2. The definition of the angles $\chi$, $\psi$, $\xi$ and $\phi$.

of two terms

$$\Phi(z) = [z(\chi - \psi)/d + (\chi + \psi)/2] + \xi\cos(\pi z/d). \tag{13}$$

The first term approximates the director distribution resulting from the actual values of the boundary angles $\chi$ and $\psi$ (for $z = d/2$ and $z = -d/2$ respectively). The deviation from this distribution is described by the second term. Its form is limited to the first Fourier component with amplitude $\xi$. This approximate expression possesses all of the essential features of the real distribution and is sufficient for qualitative considerations based on catastrophe theory. The material is characterized by the smectic C tilt angle, $\omega$, the spontaneous polarization, $P$, the dielectric anisotropy, $\Delta\varepsilon$, and the perpendicular component of the dielectric constant $\varepsilon_\perp$. A single elastic constant, $B$, is assumed.

The total free energy per unit area of the layer is now given by

$$\begin{aligned} G = \frac{1}{2}\int_{-d/2}^{d/2} \Big\{ & B(d\Phi/dz)^2 - \varepsilon_0\Delta\varepsilon E^2\sin^2\omega\sin^2\Phi - 2PE\cos\Phi \\ & - \frac{P^2}{\varepsilon_0\varepsilon_\perp}\left[\left(\int_{-d/2}^{d/2}\cos\Phi\,dz\right)^2 - \cos^2\Phi\right]\Big\}dz \\ & - \gamma_1(\cos^2\chi + \cos^2\psi) - \gamma_2(\cos\chi - \cos\psi). \end{aligned} \tag{14}$$

In this expression the dependence of the dielectric permittivity on $z$ is neglected, where convenient, $\varepsilon_{zz} = \varepsilon_\perp$; this is justified for low dielectric anisotropy. With this assumption, the voltage $U$ applied across the layer can be expressed as $U = Ed$.

### 4.1. *Structure stabilized by polar surface interactions*

The polar surface interactions result in the spontaneous splay of the polarization vector, as proposed in [4]. Two sets of critical points of the function $G$ can be distinguished. The first corresponds to the uniform director field: $\chi = 0$, $\psi = 0$, $\xi = 0$ and the second is due to the splayed state. Unfortunately the critical values of the angles $\chi$, $\psi$, $\xi$ cannot be found analytically in the latter state. In consequence, its

deformations cannot be described by means of the approach adopted here. Therefore, in order to investigate the behaviour of the layer, the function $G$ is expanded in a Taylor series in the vicinity of only one critical point determined by $\chi = \psi = \xi = 0$. Only the even powers are present in this expansion.

The determinant of the second derivative matrix vanishes for some sets of parameters and so the critical point $\chi = \psi = \xi = 0$ is degenerate. The critical values of the electric field, $E_c$, are the most interesting critical parameters. The values of $E_c$ near $E = 0$ play the role of threshold field strengths for the deformations. The equations, from which the diagonalization matrix and the threshold fields can be derived, are of third degree and can only be solved numerically. The threshold field may be negative (downward) or positive (upward) or there may be two thresholds with both signs.

The behaviour of the system results from the balance of electric, elastic and surface forces. Several distinct types of deformation can be distinguished; they are shown in figures 3, 4 and 5. In figure 3, the curves for $\chi(U)$ and $\psi(U)$ are constructed according to the relations resulting from the symmetry of the layer,

$$\chi(U) = \pi - \psi(-U). \tag{15}$$

The curve for $\chi(U)$ can be obtained from $\psi(U)$ by turning it upside-down. The curves show the angle at the bottom plate, $\psi(U)$, and the angle in the middle of the layer, $\phi(U) = [\chi(U) + \psi(U)]/2 + \xi(U)$. The plots are symmetric about the axes $\psi = 0$ and $\phi = 0$. Only the positive deformations are shown and the extremes other than the minima are omitted.

In our approach, only the behaviour in the vicinity of the critical point defined by $\chi = \psi = \xi = 0$ and $E = E_c$ is predicted correctly. The deformation of the splayed

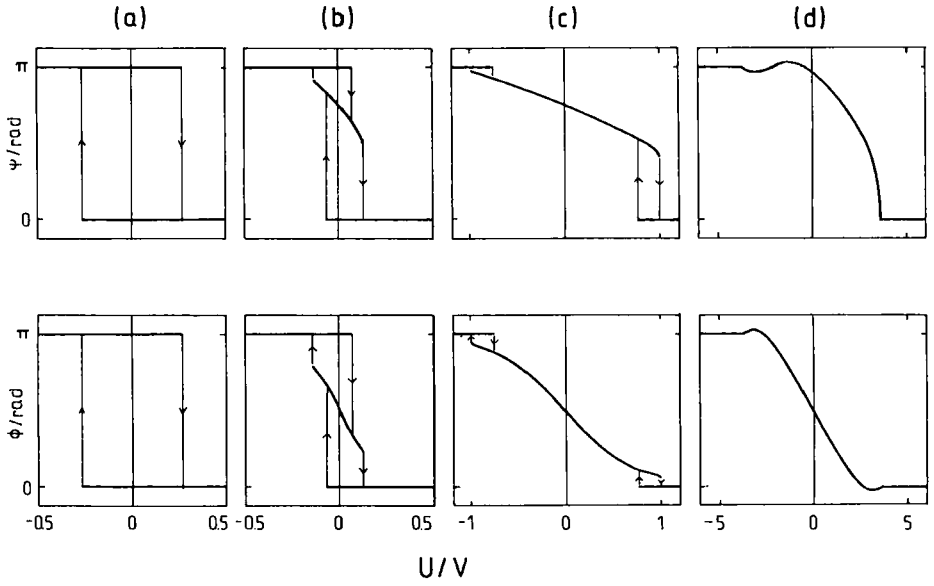


Figure 3. The deformation angles at the lower boundary plate, $\psi$, and in the middle of the layer, $\phi$, as a function of the applied voltage. $B = 2 \times 10^{-12}$ N, $P = 1 \times 10^{-5}$ C/m$^2$, $\gamma_1 = 1 \times 10^{-6}$ N/m, $\omega = 0{\cdot}4$ rad, $d = 2 \times 10^{-6}$ m, $\Delta\varepsilon = -2$ and $\varepsilon_\perp = 6$. (*a*) $\gamma_2 = 1 \times 10^{-6}$ N/m; (*b*) $\gamma_2 = 2{\cdot}5 \times 10^{-6}$ N/m; (*c*) $\gamma_2 = 5 \times 10^{-6}$ N/m; (*d*) $\gamma_2 = 1 \times 10^{-5}$ N/m, $\gamma_1 = 2 \times 10^{-7}$ N/m.

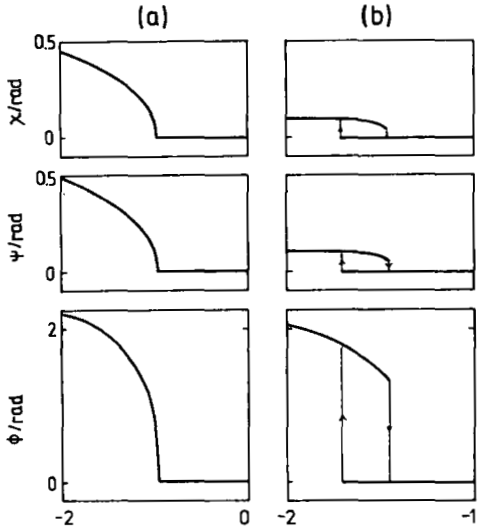


Figure 4. The deformed state realized without bistability (*a*) and with bistability (*b*). $B = 2 \times 10^{-12}$ N, $P = 1 \times 10^{-5}$ C/m$^2$, $\omega = 0{\cdot}4$ rad, $\gamma_2 = 1 \times 10^{-6}$ N/m, $d = 2 \times 10^{-6}$ m and $\varepsilon_\perp = 8$. (*a*) $\gamma_1 = 3 \times 10^{-5}$ N/m, $\Delta\varepsilon = -4$; (*b*) $\gamma_1 = 1 \times 10^{-5}$ N/m, $\Delta\varepsilon = -2$. The same curves serve as an illustration of the deformation for $\gamma_2 = 0$.

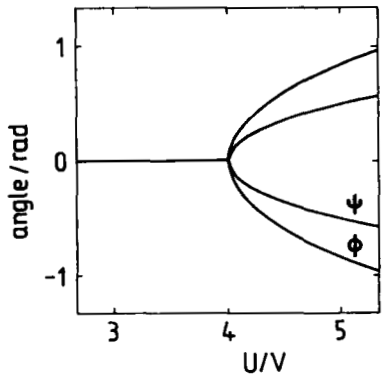


Figure 5. The dependence of the dielectric deformation on the voltage. $B = 2 \times 10^{-12}$ N, $P = 1 \times 10^{-5}$ C/m$^2$, $\Delta\varepsilon = 4$, $\omega = 0{\cdot}4$ rad, $\gamma_1 = 1 \times 10^{-6}$ N/m, $\gamma_2 = 0$, $d = 2 \times 10^{-6}$ m and $\varepsilon_\perp = 8$.

state cannot be investigated. In some cases however, the splayed state and its development are revealed by the curves calculated for the critical point considered.

The uniform state is obtaned in the field strength range in which the set of inequalities

$$a_{200} > 0, \tag{16}$$

$$4a_{200}a_{020} - a_{110}^2 > 0, \tag{17}$$

$$\det\begin{bmatrix} 2a_{200} & a_{110} & a_{101} \\ a_{110} & 2a_{020} & a_{011} \\ a_{101} & a_{011} & 2a_{002} \end{bmatrix} > 0, \tag{18}$$

is satisfied. For $E = 0$ this set is reduced to the condition

$$4B\gamma_1/d + 4\gamma_1^2 - \gamma_2^2 > 0 \tag{19}$$

which ensures the stability of the uniform state in the absence of the field, and is equivalent to the relation found earlier [5, 10].

The switching transitions occur between two uniform states with opposite directions of **P**. Several variants of this transition are possible; the examples are shown in figure 3 where they are ordered according to increasing $\gamma_2$. The curves for the splayed state are approximate and acceptable only near the thresholds; their central parts have only illustrative significance. The following properties of the system can be distinguished, starting from low values of $\gamma_2$.

(i) The uniform state can be absolutely stable. No information on the stability of the splayed state can be obtained. The following set of parameters gives an example: $B = 2 \times 10^{-12}$ N, $P = 10^{-6}$ C/m, $\gamma_1 = 10^{-5}$ N/m, $\gamma_2 = 10^{-6}$ N/m, $\omega = 0{\cdot}4$ rad, $d = 2\,\mu$m, $\Delta\varepsilon = -2$ and $\varepsilon_\perp = 8$.

(ii) Switching between uniform states can occur directly, (see figure 3 (*a*)).

(iii) The splayed state may be attained from the uniform state (see figures 3 (*b*), (*c*), (*d*)). For moderate $\gamma_2$, tristability is predicted in the absence of the field: two uniform states and the splayed state are stable (see figure 3 (*b*)). For higher $\gamma_2$, the discontinuous transition is possible (see figure 3 (*c*)). This case corresponds to the situation considered in [4, 5]. The hysteresis can disappear by suitable relation between $\gamma_1$ and $\gamma_2$ (see figure 3 (*d*)).

(iv) The unidirectional transition from the uniform state to the splayed state may occur at the critical field if the polar surface interactions are sufficiently strong. It may happen only once, since the splayed state is stable at any field. Such a property is suggested by the results obtained, but should be verified by another method, since the present approach is not applicable far from the critical points.

(v) The uniform state is unstable at any field and only the splayed state is realized. This situation occurs for strong polar interactions, e.g. if $B = 2 \times 10^{-12}$ N, $P = 10^{-5}$ C/m$^2$, $\gamma_1 = 10^{-6}$ N/m, $\gamma_2 = 10^{-4}$ N/m, $\omega = 0{\cdot}4$, $d = 2\,\mu$m, $\Delta\varepsilon = 5$ and $\varepsilon_\perp = 8$.

Another type of deformation leads from the uniform state to the deformed one, which relaxes after removing the field. This takes place if $\gamma_1$ is sufficiently high. The transition can be continuous (see figure 4 (*a*)) or discontinuous (see figure 4 (*b*)).

Figure 5 shows the transition due to the dielectric coupling which takes place if $\Delta\varepsilon > 0$. The deformations always develop continuously according to the cusp catastrophe.

### 4.2. *Structure stabilized by non-polar surface interactions*

If the polar forces can be neglected, $\gamma_2 = 0$, the director field is uniform in the undeformed sample. There exists only one critical point $\chi = 0$, $\psi = 0$, $\xi = 0$; it is degenerate, as $\det \mathbf{H} = 0$ at some electric fields $E_c$. Their values can be obtained analytically from the equation $\det \mathbf{H} = 0$ although it is of fourth order in $E$, but the solutions have a rather complicated form

$$E_c = \{P \pm \sqrt{[(P - 4\varepsilon_0 \Delta\varepsilon \sin^2 \omega X)]}\}/(2\varepsilon_0 \Delta\varepsilon \sin^2 \omega), \tag{20}$$

where

$$X = \frac{-\pi^2 B/2 - 2d\gamma_1 \pm Y}{(1 - 8/\pi^2)\, d^2} \tag{21}$$

and

$$Y = 4\sqrt{[\pi^4 B^2/4 + (32 - 2\pi^2)\, B\, d\gamma_1 + 4d^2\gamma_1^2]}. \tag{22}$$

The solutions exist if

$$\varepsilon_0 \Delta\varepsilon \sin^2\omega > (1 - 8/\pi^2)\, P^2 d^2/(-2\pi^2 B - 8d\gamma_1 + Y). \tag{23}$$

This means that there is no deformation if $\Delta\varepsilon \ll 0$. Three types of behaviour for the layer can be distinguished. If the dielectric anisotropy is negative, then there exists a single negative threshold. The layer can be deformed by the field directed antiparallel to the initial position of the polarization vector, whereas it remains stable under the parallel field. The deformation is due to the coupling between **P** and **E**, and occurs if this coupling prevails over the dielectrically forced stabilization. (As mentioned earlier, there is no deformation for negative dielectric anisotropy with too high a magnitude.) Depending on the relative magnitudes of $\gamma_1$, $P$, $d$ and $B$, two kinds of transitions can take place: the direct switching process to the state characterized by a reversed polarization and uniform director field (as in figure 3 (*a*)), or the transition to the deformed state which relaxes after the field is turned off (as in figure 4). The deformed state can arise continuously or discontinuously; the corresponding $\psi(U)$ and $\phi(U)$ functions do not differ from the curves shown in figures 4 (*a*), (*b*).

The properties of the dielectric transitions are the same as we have seen previously.

### 4.3. *The dependence of the threshold field on the system parameters*

The parameters of the system have a significant influence on the values of the thresholds. Two kinds of surface conditions are chosen and characterized here.

#### 4.3.1. *Significant polar interactions:* $\gamma_2 = 5 \times 10^{-5}$ N/m

The critical field for the transition from the uniform state to the splayed state, which is shown in figures 3 (*c*), (*d*), is considered. The results are illustrated in figures 6 (*a*), (*e*). This type of transition occurs for specific ranges of parameters. Some rules concerning the influence of the parameters can be formulated. The critical field strength is inversely proportional to $P$. It is very sensitive to surface interactions and the elastic constant. For thick layers the threshold is inversely proportional to $d$. For thin layers, for a stiff material, or for high $\gamma_1$ the threshold tends to zero, because the transition tends towards the type shown in figure 3 (*b*). The situation described in §4.1 (iv) may also prevent the transition. Examples of this effect, marked by circles ending the curves, can be seen in figures 6 (*b*), (*d*),(*e*) for low $P$, high $\gamma_1$, or low $B$. The transition may also become impossible if the high value of $\Delta\varepsilon > 0$ results in a loss of stability of the uniform state (see figure 6 (*c*)).

These results can be compared to similar data presented in [10]. The evident discrepancy may be due to the fact that in [10] the splayed state was assumed for $\gamma_2 = 0$.

#### 4.3.2. *Negligible polar interactions:* $\gamma_2 = 0$

Figures 7 (*a*)–(*e*) show the threshold as a function of the parameters for all types of deformation due to the spontaneous polarization. As the field strength is negative,

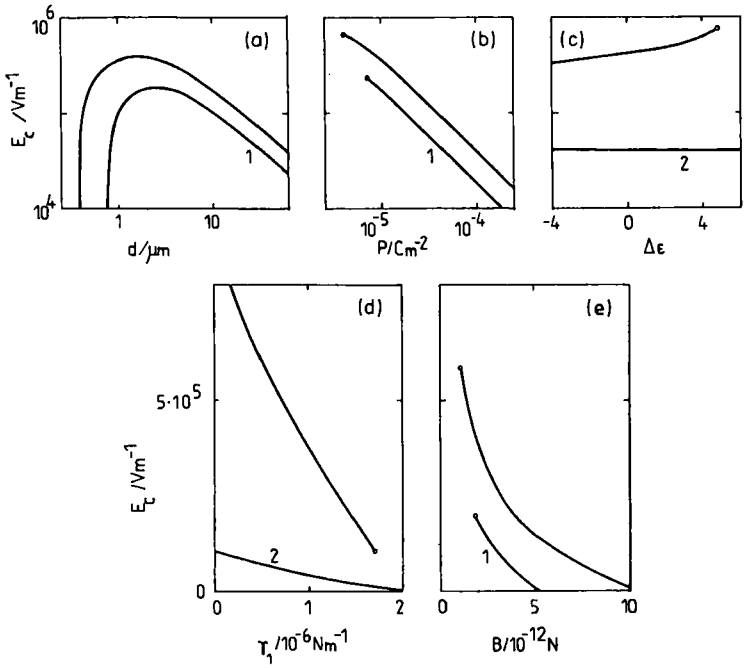


Figure 6. The threshold field for the transition between uniform and splayed states as a function of the parameters. The following set of parameters was used if not indicated elsewhere in the figures: $B = 2 \times 10^{-12}$ N, $P = 1 \times 10^{-5}$ C/m$^2$, $\Delta\varepsilon = -2$, $\omega = 0{\cdot}4$ rad, $\gamma_1 = 1 \times 10^{-6}$ N/m, $\gamma_2 = 5 \times 10^{-5}$ N/m, $d = 2 \times 10^{-6}$ m and $\varepsilon_\perp = 6$. 1, $\gamma_1 = 1{\cdot}5 \times 10^{-6}$ N/m; 2, $P = 1 \times 10^{-4}$ C/m$^2$.

its absolute value is plotted. The following approximate relations can be found: $|E_c| \sim \gamma_1$ for small $\gamma_1$, $|E_c| \sim 1/P$ for high $P$, and $|E_c| \sim d^{-n}$, where $n \approx 1$–$1{\cdot}5$ depending on the surface energy. The threshold decreases with $\Delta\varepsilon$ and increases with $B$; the last dependence is minor for low $\gamma_1$. In some cases the transitions are impossible, these are marked by circles on the ends of the curves. The most interesting switching occurs for stiff materials with moderate polarization, weakly anchored at the boundaries and confined in a layer of moderate thickness. The threshold for dielectric deformation is almost independent of $\gamma_1$, proportional to $P$ (for high $P$), and very high for small $\Delta\varepsilon$.

## 5. Tilted smectic layers

The smectic layers may not be ideally perpendicular to the boundary plates but slightly tilted, making an angle $\alpha$ with the normal to the plates. Because of the equality of the angles $\chi$ and $\psi$, the free energy $G$ can be treated as a function of two variables, $\psi$ and $\xi$, which define the azimuthal angle $\Phi(z)$

$$\Phi(z) = \psi_0 + \psi + \xi \cos(\pi z/d), \tag{24}$$

where $\psi_0$ denotes the initial value of $\Phi$ resulting from the geometric relation

$$\sin\psi_0 = \tan\alpha/\tan\omega. \tag{25}$$

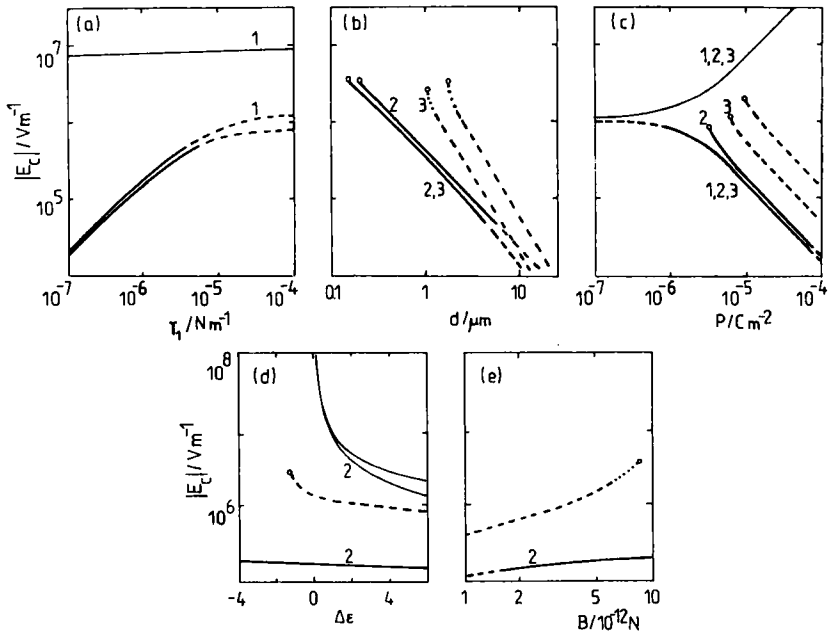


Figure 7. The absolute value of the threshold field for non-polar surface interactions. The following set of parameters is used if not indicated elsewhere in the figures: $B = 6 \times 10^{-12}$ N, $P = 1 \times 10^{-5}$ C/m$^2$, $\Delta\varepsilon = -1$, $\omega = 0{\cdot}4$ rad, $\gamma_1 = 1 \times 10^{-4}$ N/m, $\gamma_2 = 0$, $d = 2 \times 10^{-6}$ m and $\varepsilon_\perp = 6$. Full line, switching; dashed line, continuous deformations; dotted line, deformations with hysteresis; thin line, dielectric deformations. 1, $\Delta\varepsilon = 1$; 2, $\gamma_1 = 1 \times 10^{-6}$ N/m; 3, $B = 2 \times 10^{-12}$ N.

In order to simplify and shorten the calculations, the influence of the polarization charge is neglected, and the free energy per unit area, $G$, is expressed as

$$G = \int_{-d/2}^{d/2} \{B(d\Phi/dz)^2 - 2qB\sin\alpha(d\Phi/dz) + Bq^2 - \Delta\varepsilon\varepsilon E^2(\cos\omega\sin\alpha - \sin\omega\sin\Phi\cos\alpha)^2 - 2PE\cos\Phi\cos\alpha\}\, d_z - 2\gamma_1\cos^2(\psi_0 + \psi)\cos^2\alpha. \quad (26)$$

Its expansion in a Taylor series contains the even powers as well as the odd. As previously, the normalization reduces this expansion to the form with one essential variable, equivalent to the butterfly catastrophe. The results are exemplified in figure 8 (*a*) for the case of switching. The small deformation exists also in the absence of the field and the threshold character of the switching is retained. The transitions to the deformed state are continuous. The dielectric transitions are continuous too, as shown in figure 8 (*b*).

## 6. Concluding remarks

In this paper, the bulk deformations of the director field were considered by using a one dimensional model. The effect of switching was treated as the rotation of the director. Its distribution was assumed to take the simplified form given by equation (13). The effect of this type can take place if the surface interactions are not too strong. Only under this assumption can the switching be described by equation (13). In the

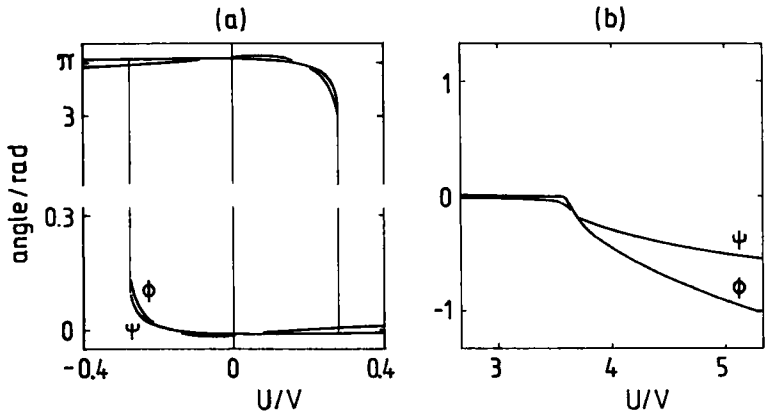


Figure 8. The effect of the tilt angle $\alpha = 0{\cdot}01$ rad, $B = 2 \times 10^{-12}$ N, $P = 1 \times 10^{-5}$ C/m$^2$, $\omega = 0{\cdot}4$ rad, $\gamma_1 = 1 \times 10^{-6}$ N/m, $\gamma_2 = 0$, $d = 2 \times 10^{-6}$ m. (*a*) the switching transition $\Delta\varepsilon = -2$; (*b*) the dielectric transition $\Delta\varepsilon = 4$.

opposite case other kinds of distortion take place. The significance of this limitation is illustrated by the results shown in figure 7.

A variety of transitions induced by the electric field in ferroelectric liquid crystal layers can be predicted on the basis of the stationary states found in this work. The results have a qualitative character; this is inherent in the method based on catastrophe theory. Only the critical points and their neighbourhoods are determined correctly, although this is sufficient to predict the behaviour of the system in most cases. The results correspond to the behaviour found in earlier work (e.g. [4, 5]).

The calculations for a function of three variables are much more laborious than for a function of two variables. The complexity of the calculus increases drastically, if the tilt of the smectic layers is introduced. Odd terms appear in the Taylor expansion and all of the coefficients are more complicated. Therefore the tilt is only considered if $\gamma_2 = 0$, when two variables are sufficient.

The strong polar surface interactions should result in the chevron structure, which seems to require six variables for complete modelling of the deformation. Therefore the sharp bending of the smectic layers due to this structure is ignored here. Nevertheless the stationary states predicted for flat layers are analogous to the states occurring in the chevron structure. This analogy was utilized by Hiji *et al.* in [19]. It can be applied also to the case of switching between three stable states observed by Johno *et al.* [20]. The role of the tilt in the polar interaction case, e.g. in the chevron structure, can be predicted on the basis of the results presented in §5. The curves are rounded smoothly, and in some cases the transitions became continuous.

The chiral smectic C structure was assumed to be unwound by the surface interaction. Because of this assumption the chirality $q$ does not enter in the coefficients of the Taylor expansion.

In some work, the role of the polarization space charge was discussed (e.g. in [7, 8]). This charge manifests itself by the lowering of the electric field required for the transition from the splayed state to the uniform state, and, in some cases, by destabilization of the splayed state. These effects were found here in agreement with [7]. The critical field strengths and the condition (19) are not affected by the charge.

The method applied in this paper leads to elementary but sometimes rather large expressions, resulting from the normalization procedure of the Taylor series. Numerical

calculations are necessary to obtain their values. The analytical formulae for the coefficients $a_i$ would be instructive but using them is impractical because of their complexity. However, even the numerical route yields useful systematization of the possible types of stationary states.

## References


[1] CLARK, N. A., and LAGERWALL, S. T., 1980, *Appl. Phys. Lett.*, **36**, 899.
[2] SCHILLER, P., PELZL, G., and DEMUS, D., 1987, *Liq. Crystals*, **2**, 21.
[3] NAKAGAWA, M., 1989, *Molec. Crystals liq. Crystals*, **174**, 65.
[4] HANDSCHY, M. A., and CLARK, N. A., 1983, *Phys. Rev. Lett.*, **51**, 471.
[5] HANDSCHY, M. A., and CLARK, N. A., 1985, *Ferroelectrics*, **59**, 69.
[6] NAKAGAWA, M., and AKAHANE, T., 1986, *J. phys. Soc. Japan*, **55**, 1516.
[7] NAKAGAWA, M., and AKAHANE, T., 1986, *J. phys. Soc. Japan*, **55**, 4492.
[8] PAUWELS, H., DE MEY, G., REYNAERTS, C., and CUYPERS, F., 1989, *Liq. Crystals*, **4**, 497.
[9] KIMURA, S., NISHIYAMA, S., OUCHI, Y., TAKEZOE, H., and FUKUDA, A., 1987, *Jap. J. appl. Phys.*, **26**, L255.
[10] NONAKA, S., ITO, K., ISOGAI, M., and ODAMURA, M., 1987, *Jap. J. appl. Phys.*, **26**, 1609.
[11] NAKAGAWA, M., ISHIKAWA, M., and AKAHANE, T., 1988, *Jap. J. appl. Phys.*, **27**, 456.
[12] NAKAGAWA, M., 1989, *Molec. Crystals liq. Crystals*, **173**, 1.
[13] OUCHI, Y., TAKANO, H., TAKEZOE, H., and FUKUDA, A., 1987, *Jap. J. appl. Phys.*, **26**, L21.
[14] SATO, Y., TANAKA, T., KOBAYASHI, H., AOKI, K., WATANABE, H., TAKESHITA, H., OUCHI, Y., TAKEZOE, H., and FUKUDA, A., 1989, *Jap. J. appl. Phys.*, **28**, L483.
[15] POSTON, T., and STEWART, I., 1976, *Taylor Expansions and Catastrophes* (Pitman).
[16] DERFEL, G., 1988, *Liq. Crystals*, **3**, 1411.
[17] DERFEL, G., 1989, *Liq. Crystals*, **6**, 293.
[18] DERFEL, G., 1989, *Liq. Crystals*, **6**, 709.
[19] HIJI, N., OUCHI, Y., TAKEZOE, H., and FUKUDA, A., 1988, *Jap. J. appl. Phys.*, **27**, 8.
[20] JOHNO, M., CHANDANI, A. D. L., OUCHI, Y., TAKEZOE, H., FUKUDA, A., ICHINASHI, M., and FURUKAWA, K., 1989, *Jap. J. appl. Phys.*, **28**, L119.